

THE UNIVERSITY OF ARIZONA
GRADUATE COLLEGE

As members of the Master’s Committee, we certify that we have read the report prepared by Madeline Bergay, titled “Multi-line Triangulation 3D Imaging for Educational Applications” and recommend that it be accepted as fulfilling the dissertation requirement for the Master’s Degree.



Florian Willomitzer

Date: 05/11/23



Tom Milster

Date: 05/10/2023



/Hong Hua/ (May 9, 2023 21:49 PDT)

Hong Hua

Date: 05/09/2023

Final approval and acceptance of this report is contingent upon the candidate’s submission of the final copies of the thesis to the Graduate College.

I hereby certify that I have read this report prepared under my direction and recommend that it be accepted as fulfilling the Master’s requirement.



Florian Willomitzer
Master’s Thesis Committee Chair
College of Optical Sciences

Date: 05/11/23



ARIZONA

Multi-line Triangulation 3D Imaging for Educational Applications

By

Madeline Bergay

Copyright © Madeline Bergay 2023

A Master's Report Submitted to the Faculty of the

WYANT COLLEGE OF OPTICAL SCIENCES

In Partial Fulfillment of the Requirements

For the Degree of

MASTER OF SCIENCE

In the Graduate College

THE UNIVERSITY OF ARIZONA

2023

ABSTRACT

Line triangulation is a fast, efficient, and highly accurate 3D imaging technique that projects lines onto an object's surface and captures the distorted pattern using a camera to calculate the 3D coordinates. The system outlined in this paper utilizes projected multi-line triangulation and is designed to be cost-effective, utilizing readily available materials, as well as visually intuitive, making it well-suited for educational purposes. The system can employ three different image acquisition techniques: no scanning, object scanning, and line scanning. No scanning allows for quick data capture in a single shot with low point cloud density. Object-scanning and line-scanning can be used to fill in the gaps but require more images. Depths – the z coordinates of the (x,y,z) point cloud - are calibrated differently depending on imaging method. No scanning and object scanning both use a calibration curve to fit the data, while line scanning uses a calibration plane. An accuracy test was conducted by imaging a planar surface at a known depth using both the calibration curve and calibration plane methods. When tested at a specific plane, the calibration curve had a standard deviation of 0.98 mm, and the calibration plane method had a standard deviation of 0.66 mm. The system was able to generate 3D point clouds of various objects using all methods. All methods provide data capable of creating point clouds with centimeter precision.

Table of Contents

1. Introduction	3
1.2 Coordinate System	3
2. Performance Factors	4
3. Types of 3D Imaging	5
4. Method	9
4.1 Concept	9
4.2 Image Acquisition	10
4.2.1 No scanning	11
4.2.2 Object Scanning	11
4.2.3 Line Scanning	11
4.3 Materials	12
4.4 Setup	13
4.5 Image Acquisition	14
4.5.1 No Scanning Image Acquisition	14
4.5.2 Object Scanning Image Acquisition	15
4.5.3 Line Scanning Image Acquisition	15
4.6 Image Processing	15
4.7 Callibration	17
4.7.1 Object Shifting Callibration	17
4.7.2 Line Shifting Callibration	18
4.8 Object Fitting	19
4.8.1 Object Fitting with No Shifting	20
4.8.2 Object Fitting with Object Shifting	20
4.8.3 Object Fitting with Line Shifting	20
5. Results	21
5.1 3D Point Clouds	21
5.1.1 Single Shot Point Cloud	22
5.1.2 Comparing Object-Shifted and Line-Shifted Point Clouds	23
5.1.3 Line Shifted Point Cloud	24
5.2 Calibration Line vs. Calibration Plane Error	26
6. Conclusion	28
7. References	29

1. Introduction

Line triangulation is a simple, yet effective type of 3D imaging. It operates on principles that are similar to those employed by the human visual system to perceive depth. For humans, the ability to determine depth is a result of having two eyes, or detectors, that capture slightly different images with distinct viewing angles. When the human brain finds matching points in these images, it creates a seamless 3D representation of the scene. Line triangulation works similarly to this; however, it involves projecting a set of lines onto the object and then using a camera to capture the pattern of the lines as they intersect the object's surface [1]. By analyzing the distortion of the laser line pattern, the camera and software can calculate the 3D coordinates of the points at the line-object intersection. With this data, a point cloud is produced, where each point in the cloud represents a specific location on the object's surface, defined by its x, y, and z coordinates in 3D space.

This technology has a wide range of applications including: the medical field creating 3D models of organs, robotics, and self-driving cars for mapping environments, in smart devices for facial recognition and depth detection, and entertainment for creating immersive virtual reality experiences. Overall, line triangulation has enabled 3D imaging that is fast, efficient, and highly accurate [2].

3D imaging is a rapidly growing market. In 2021, the worldwide 3D sensor market had a size of \$17,607.9 million, and it is anticipated to increase at a compound annual growth rate of 13.0% to attain a projected revenue of \$56,992.3 million by 2031 [3]. Because of this, there is a growing demand for professionals with experience in 3D imaging. This paper describes a system for projected multi-line triangulation designed to be affordable, made from easily accessible materials such as a classroom projector and a cell phone camera, and to be visually intuitive, making it ideal for educational applications.

1.2 COORDINATE SYSTEM

Throughout this paper the coordinate system shown in Figure 1 is used.

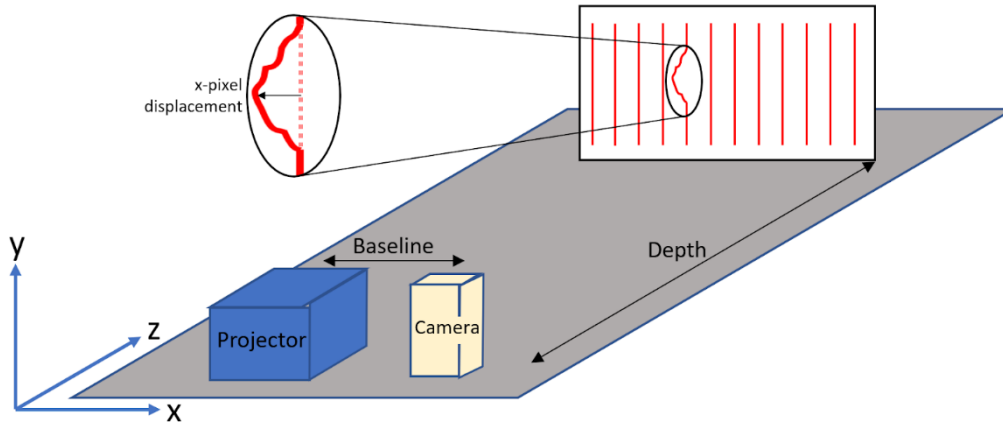


Figure 1: Diagram describing the coordinate system as well as various measurements used throughout this paper.

Where depth is the distance along the z-axis, and pixel displacement is along the x-axis.

2. Performance Factors

Common factors for evaluating 3D imaging methods include depth resolution, point density, point cloud error, depth of field, field of view, illumination variability, simplicity, and accessibility.

Depth resolution refers to the smallest change in distance that can be detected by an imaging system, and it is typically expressed in units of length. This paper uses the phrase “high precision” depth resolution when referring to a micron level depth resolution, and a “low precision” depth resolution referring to millimeter level depth resolution.

Point density indicates the concentration of points in the final point cloud. This density is relative to the resolution of the detector and can be expressed in lines/ potential pixels. The potential pixel value characterizes the pixel value of the sensor. Oftentimes systems will have a different vertical and horizontal point density.

Point cloud accuracy refers to how closely the 3D points in a point cloud correspond to the actual 3D geometry of the object being imaged.

Depth of field specifies the range of depth from the camera at which an object will appear in focus for an accurate measurement. Field of view denotes the area that is being imaged. The field of view of the system is limited by the camera's field of view and the projector's field of view.

Illumination variability describes the variety of lighting conditions that the system may operate effectively. A system with high illumination variability will work in both dark, indoor environments and bright, outdoor environments. A system with low illumination variability may have higher point cloud error in bright lighting due to low contrast.

Simplicity refers to how intuitive the system is. A system with higher simplicity will be easier to understand, even for people with little to no knowledge in the field. This parameter is especially important when designing systems for educational purposes.

Accessibility includes the cost and availability of materials in the system. This is also an important factor to consider when designing systems with educational value. A system with higher accessibility will be made with low-cost and/ or readily available materials.

3. Types of 3D Imaging

There are many types of 3D imaging utilizing triangulation. Stereo vision is the 3D imaging method most similar to the human visual system. Stereo vision uses two cameras to capture 2D images of the same object from two different angles. These images are then processed through a correlation algorithm to determine the correspondence between the two images. By triangulating the position between the two cameras, a 3D point cloud can be obtained. Stereo vision has many benefits, including fast image acquisition, a large field of view, and lighting variability without requiring any additional artificial pattern. However, stereo vision also has disadvantages, mainly image quality. The correlation method can be process-intensive and often requires block averaging, which results in a loss in point density. In featureless regions, it can also be challenging to find corresponding points, leading to holes in the point cloud and point cloud errors [4].

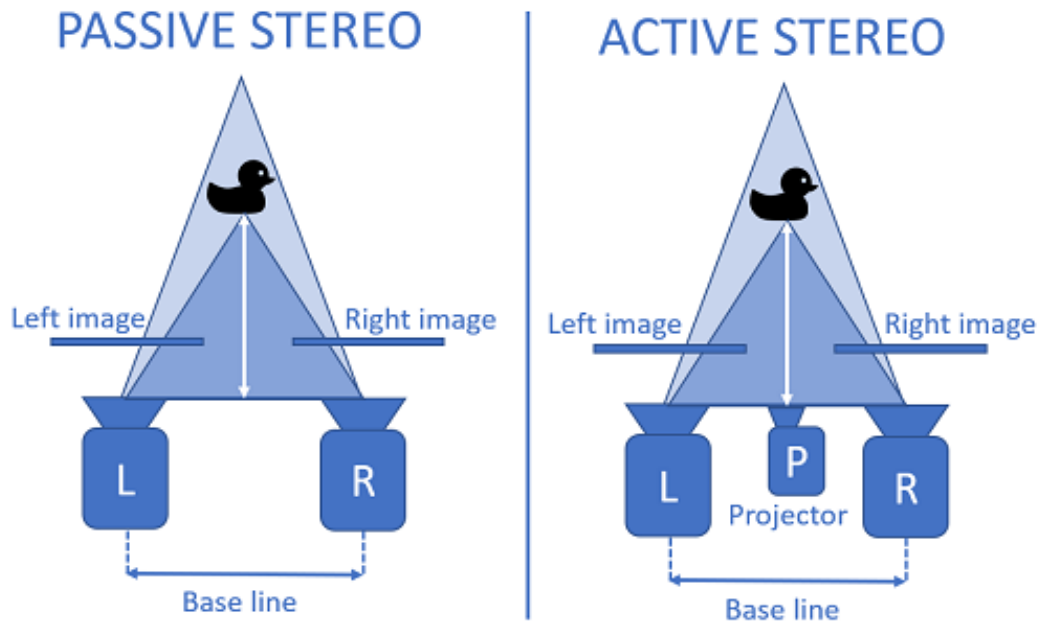


Figure 2. Diagrams for passive stereo (left), active stereo (center) and structured light (right). [5] Passive stereo utilizes two cameras, capturing a left and right image of the same object. Active stereo adds an additional pattern projector to increase uniqueness. Structured light removes one of the cameras and instead utilizes a known image being projected.

To increase the feature uniqueness, a pattern projector can be added, removing the reliance on object features. This technique is referred to as active stereo vision. Although it results in better image quality than stereo vision, it has worse lighting variability and depth of field. Furthermore, adding additional components such as the pattern projector adds to the cost, complexity, overall size, and therefore accessibility of the system [4].

If a known structured pattern is used instead of a random pattern, only one camera is necessary because the image at the location of the projector is equivalent to the pattern being projected, as shown in Figure 3. This requires fewer components than the previous method and is less processing-intensive than the passive stereo technique because there is no correspondence processing. Unfortunately, limitations like point density and point cloud errors still exist when there are features in the structure that cannot be located or distinguished. Additional measurement errors or missing data could result from shiny or specular surfaces [4].

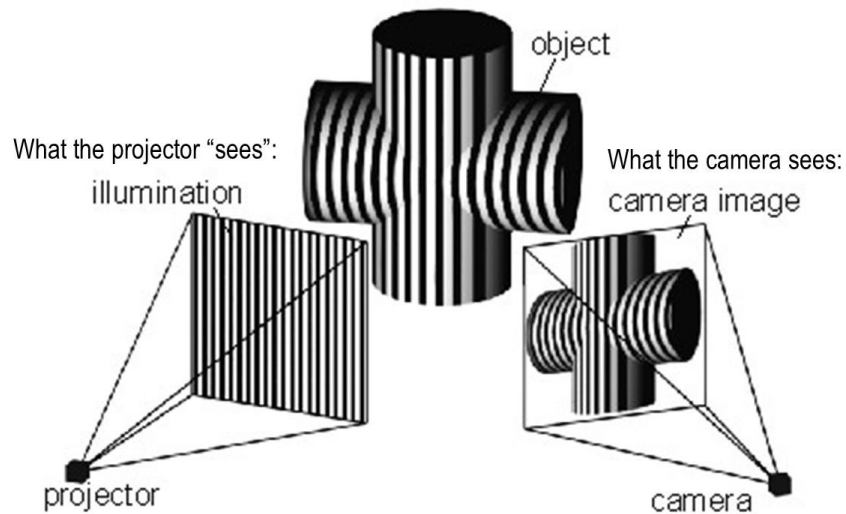


Figure 3. Diagram for Active Stereo 3D imaging with structured light. [6] This method utilizes a projector and camera. Only one camera is needed for this method because if a camera was placed at the location of the projector, it would image the same illumination pattern.

To further simplify the system, the structured pattern projection can be replaced by a laser line, which is referred to as laser-line triangulation. This technique involves projecting a single line onto an object and imaging the deviated reflection. The reflection off of the object will result in a displaced laser line that is proportional to the depth of the object [7]. A calibration is completed to map the line displacement to the depth of the object. To obtain the geometric shape of the entire object, the object can be translated across the beam. This will result in a series of profiles that can be combined to get a point cloud representation of the full geometry.

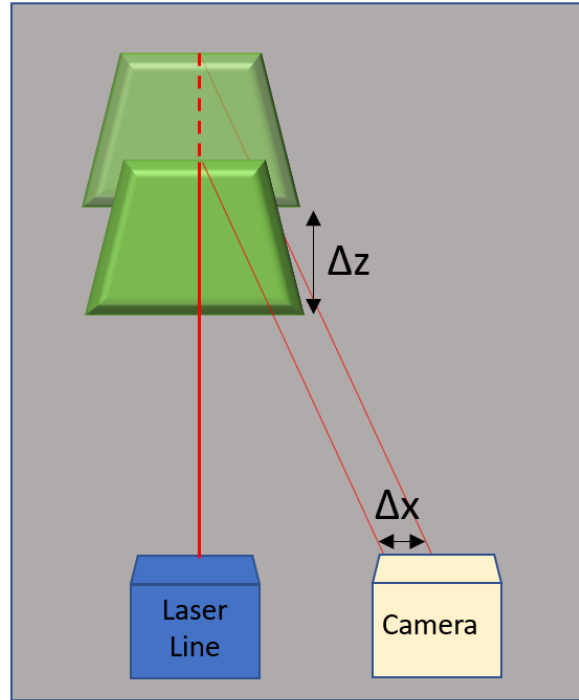


Figure 4. Diagram demonstrating the relationship between the object shift Δz and pixel shift Δx for laser-line triangulation.

Laser-line triangulation works under high illumination variability due to the powerful, monochromatic nature of the laser. It also utilizes a simpler measurement principle, eliminating the correspondence errors of stereo vision and the point cloud errors in the structured light method due to missing features. This method is very useful for conveyor applications where the object is easily translated. The biggest drawback of this technique is that it is slower and requires multiple images to be taken to obtain the entire profile of the object.

There are several ways to create 3D images using line triangulation. One method involves passing the object perpendicular to the laser line at a constant velocity while taking images at regular time intervals. By adjusting the time intervals, it is possible to change the density of the 3D point cloud. Alternatively, one can move the camera and laser simultaneously, rather than the object, which works similarly to moving the object. However, depending on the size of the object, it is often easier

to move the camera and laser instead. If the angle between the camera and the laser changes, the profile may no longer be accurate, and a new calibration is needed.

Another method is to scan the laser across the object using a rotating or scanning mirror to steer the laser line mechanically. This method is usually more convenient because a mechanical mirror is typically much lighter than the object or camera system and has fewer engineering challenges. However, it requires a new calibration to be completed each time the angle between the camera and laser changes [4].

With all methods mentioned, accuracy is highly dependent on how well the algorithm can recognize similarities between the two images. Time-coded structured light enables the capture of precise measurements with high accuracy. This method involves projecting simple patterns, such as fringes, that change over time so that each pixel has a unique time-coded structured light. This eliminates the need for block averaging, making it the most accurate method mentioned. However, it is slower as it requires multiple structured light patterns to be projected over time for each image. It also has lower simplicity [4].

This is not an exhaustive list of 3D imaging techniques. There are more unique methods as well as adaptations of these methods that are commonly used for 3D imaging.

4. Method

4.1 CONCEPT

The objective of this project was to develop an accessible 3D imaging system for educational purposes. While depth resolution is an essential factor when creating any 3D imaging system, simplicity, and accessibility are strong driving factors when designing for educational purposes. The device must be designed with the goal of visually demonstrating triangulation concepts rather than achieving high precision. With these considerations in mind, a hybrid method that combines

structured light and laser line triangulation was chosen; it is referred to as projected multi-line triangulation.

This approach projects a series of lines instead of a single line, which increases the point density obtained in a single shot and reduces the number of images needed to be captured. Unlike laser lines, this method uses projected lines, which have less illumination variability. Standard classroom projectors are less expensive and more widely available than multi-line laser projectors, and they are still capable of producing relatively thin lines. Moreover, standard classroom projectors emit lines in the visible spectrum, making it easier to see the deviated line and grasp the concept. Therefore, this method vastly improves simplicity and accessibility, making it ideal for educational applications.

To distinguish between multiple lines in this system, each line was assigned a range of pixels based on its position on the camera detector when the planar object was closest or farthest from the camera. Although assigning pixel ranges for the lines increases simplicity, it has some disadvantages. The position between the camera and the projector must remain constant, and the depth of field is more limited. Additionally, this method only works when all lines are in view and do not overlap.

4.2 IMAGE ACQUISITION

There are three different ways in which this system may be employed: without scanning, with object scanning, and with line scanning.

4.2.1 No scanning

When no scanning is used, the point cloud can be obtained in a single shot. This method is the fastest method, while still producing accurate results. The downside of this method is there are many gaps in the point cloud. The 3D profile is only known at the location of the projected lines, which leads large gaps in the point cloud, and therefore low point density across the horizontal axis.

When measuring extremely simple objects where the shape is repetitive such as a cylinder or planar surface, this method works very well.

4.2.2 Object Scanning

To fill in the gaps, the object can be scanned across the lines. This is best done using some sort of translation stage such that the object is only moving in the intended direction, and no additional tilt is added. By displaying the profiles back-to-back, the gaps are filled in, and a more complete profile of the object may be obtained. Since the object is the only feature moving, the calibration is the same as without scanning. This method has the least point cloud errors, and the horizontal point density can be tailored to the application by obtaining more or less object position images.

4.2.3 Line Scanning

Line scanning can be used for applications where it is difficult to translate the object, such as with large, living, or moving objects. This method is similar to object scanning, except that the lines are translated as little as one pixel at a time instead of the object moving. Only the image being projected, not the projector itself, is moving. However, this method has a disadvantage: when the angle between the camera and lines shifts, the calibration computation changes. The calibration computations between the lines can be extrapolated from the known values at the lines, but this results in less accuracy due to polynomial approximations.

Overall, this system is a simple and accessible way to visually demonstrate the principles of triangulation. By using a projected multi-line triangulation method, 3D point clouds of objects can be obtained while keeping costs low and ensuring ease of use.

4.3 MATERIALS

The system consists of three main components: a camera, a line projector, and a computer to run the software. The system was designed for accessibility, so there is flexibility with choosing which

camera and line projector. A phone camera can be used as the system's camera, although it is recommended that the camera has a minimum 12 MP sensor. In this setup, an iPhone 11 with a 12 MP [8] camera sensor was used. When using this camera many automatic features such as autofocus, and auto compression must be disabled. There are many cell phone applications such as “Halide” that can do this automatically [9]. The line projector must be selected such that thin, uniform, vertical lines with even spacing can be produced. In this setup, a VS250 SVGA 3LCD Projector was used, which has a resolution of 800 x 600 pixels [10]. For optimal performance, the lines were projected with a thickness of 1 pixel. The thinner the lines are, the higher the point cloud density that can be achieved.

The line projector does not necessarily have to be a classroom projector. One downside of using a classroom projector is that it is only in focus in one plane. When projecting onto a 3D object, this means that some of the lines will no longer be in focus, increasing the line thickness and blurring the appearance. The system does not require the lines to be the same size, but when the lines are thicker due to defocus, the point cloud density is more limited, and there could be additional point cloud errors. The system would also work with a laser line projector employing a diffractive optical element (DOE) to form vertical lines.

Additional materials include a planar, non-reflective viewing screen, a ruler for measurements, and a Bluetooth clicker device.

4.4 SETUP

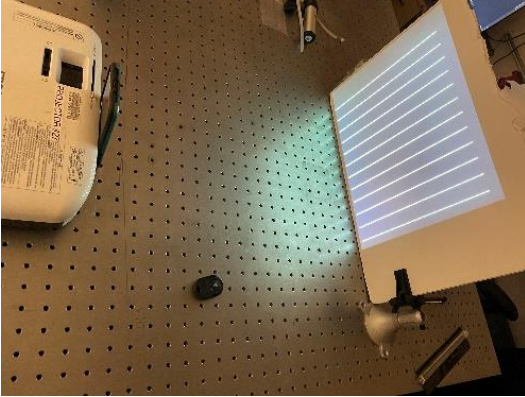


Figure 5. (Left) Picture of entire setup including projector, cell phone camera, and planar viewing screen.

Figure 6. (Right) Picture showing close up position of camera and projector.

The distance between the detector and the line projector can be referred to as the baseline. Increasing the baseline leads to each "view" being farther apart, which creates greater disparities between the two "views" and increases the depth resolution. However, this increase in depth resolution introduces limitations. Importantly, it causes the overlap between the two "views" to decrease, which limits the field of view. Another limitation is an increased minimum depth of field. Furthermore, with multi-line triangulation, the distance between the lines is limited by the baseline. For any given line on a part of the object closest to the camera, it must not overlap with the line next to it. If the lines are overlapping, this could be compensated for by increasing the distance between the lines. However, the greater the distance between the lines, the more images need to be taken to capture the entire object. Ultimately, the baseline must be chosen to maximize depth resolution without limiting the field of view or increasing the number of images needed to be taken. Therefore, the selection of the baseline distance requires careful consideration of the trade-offs between these competing factors. This relationship can be characterized in Equation 1.

$$N_L \cdot \Delta z_{Max} \cdot \tan \theta \leq \Delta X_{Max} \quad (1)$$

Here N_L is the number of lines, Δz_{Max} is the maximum depth range for the object, θ is the angle between the camera and projector, and ΔX_{Max} is the maximum distance in x that the lines can move.

ΔX_{Max} is a parameter intrinsic to the camera, and can be treated as a constant. Considering this, when the number of lines increases, either Δz_{Max} , θ or both must decrease as well.

To optimize the depth resolution of the object profile, the camera was placed 3-8 cm from the projector lens. If the camera is placed closer than 3 cm from the projector lens, the camera begins to clip the image projected. When the baseline is about 8 cm, the distance is optimized so that the lines are not overlapping, but the object profile depth resolution is still maximized. In this experiment the system utilized 12 lines, spaced 66 pixels apart.

To take photos, it is essential to keep the positions of the projector and camera constant. A Bluetooth clicker device can be used to capture the images on the phone camera without touching the phone, as touching the phone could alter the position, ruining the entire calibration.

4.5 IMAGE ACQUISITION

To calibrate the system, photos of the planar viewing screen are taken at four or more different depths, with two of the depths corresponding to the minimum and maximum range of the object depth. For all of these calibration photos, the only factor changing is the depth of the planar object. Any additional tilt or translation in the x or y direction should be avoided. The planar screen distance should be recorded and used in calibration.

4.5.1 No scanning Image Acquisition

When no scanning is used, all data can be captured in a single shot. The viewing screen should be moved to the minimum depth position. The object is placed in front of the viewing screen such that the thickest part of the object is well within the depth of field limit. From here a single image can be captured by clicking the Bluetooth clicker, and image acquisition is complete.

4.5.2 Object Scanning Method

When object scanning is used, multiple images must be acquired. With this method it is best if the object can be placed on either a translation stage or rail carrier such that the object can be shifted laterally without changing depth or rotation. The number of images required depends on the point density desired. For all images, the shift must be recorded. It is recommended that the object is shifted over a large enough distance such that one point on the object scans the entire distance between two lines. The shift between images can be scaled to the distance it takes to scan the object from one line to the next.

4.5.3 Line scanning method

The line scanning method also requires multiple images; however, the object remains stationary. Multiple line photos are used with a consistent shift between each set of lines. When the lines are 65 pixels apart, if five images are used, the lines for the second photo will be shifted by 13 pixels, the third by 26 pixels, and the fifth by 52 such that if one more shift were to occur the line would be at the location of the subsequent line. An image of the stationary object is taken with each of the shifted lines projected.

4.6 IMAGE PROCESSING

The calibration photos are stored as grayscale .bmp images along with the known z location for each photo. If any photos are not grayscale .bmp images they can be converted. To determine the precise center point of each line in each photo, first, the image is blurred vertically. This helps prevent false line edges from being detected without sacrificing precision. Edge detection is then used to determine the left and right boundaries for each line. The Laplacian of Gaussian (LoG) method is used for edge detection. First, a 2-D Gaussian smoothing kernel with a standard deviation of 20 used to filter the image is applied to reduce noise, and then the Laplacian is found. The Laplacian is a 2-D isotropic measure of the 2nd spatial derivative of an image, and by finding steep zero crossings,

finds the edges. Additionally, by examining whether the slope is positive or negative, it can be determined whether the artifact is the left or right boundary of the line.

Once the boundaries of the line are determined, additional sorting is done to ensure that all edges detected are true edges and that there are no mismatched edges. By default, the edges are sorted in the order of detection from left to right. For each pair of left/ right borders, it is checked that the left border is before the right border, the distance between the left and right borders does not approach the expected distance between the lines, and there are no two lines too close to each other.

Parameters for expected distance between lines and minimum spacing can be manually adjusted by the user. From here, the centers of each line can be determined with subpixel precision. The intensity profile within the left and right borders of each line is fit to a gaussian function, and the peak of each Gaussian function is determined to be the center of each line.

The centerline values of each line across the plane correspond to known pixel positions of the plane at that known depth. The centerlines are found for all known depth locations.

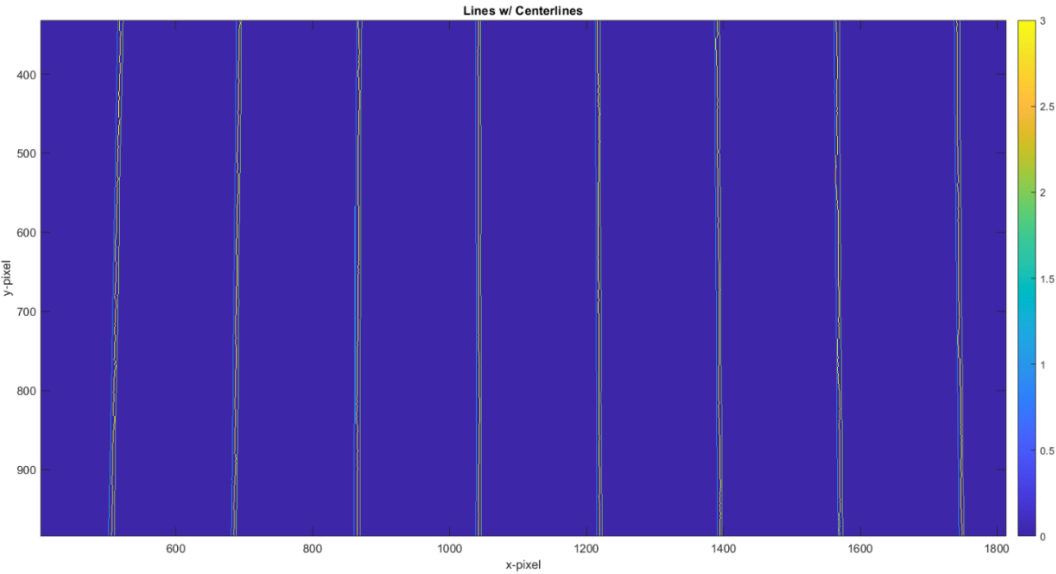


Figure 7. Simulation showing left border (=1, light blue), right border (=2, green), and center (=3, yellow) of calibration lines.

From here, calibration can be completed.

4.7 CALLIBRATION

There are two different methods that may be used to calibrate the system, depending on if no scanning, object scanning or line scanning is used.

4.7.1 Object Shifting Calibration

If no scanning or object scanning is employed, the x-pixel displacement can be directly mapped to the depth. Four or more positions are required so that a high-order polynomial can be fitted to the relationship between the pixel location and the depth. Though a calibration line could be fit with just two depths corresponding to the minimum and maximum depths, a higher-order polynomial can be fit to more locations, resulting in higher accuracy. It is recommended to take callibration photos at 4-10 different depths. A high order polynomial is created relating x-pixel displacement to z depth for every pixel on each line. This is used later to predict the z position given an x position.

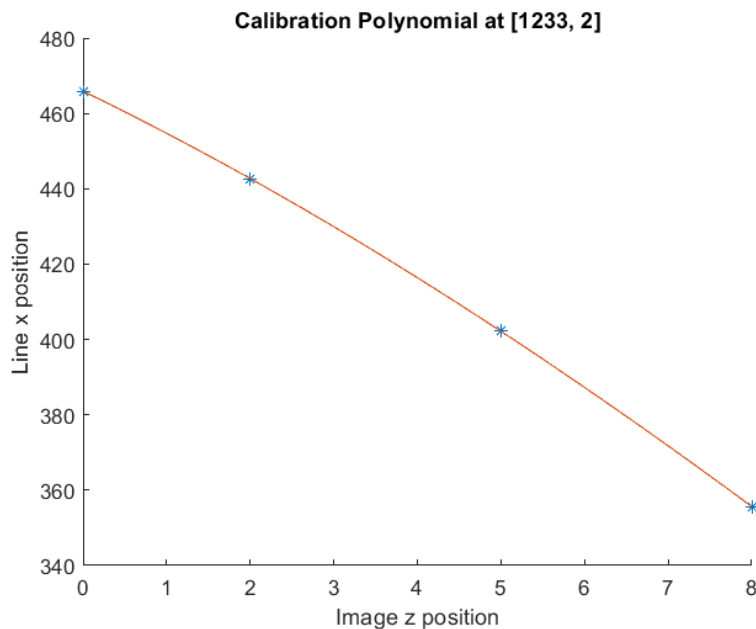


Figure 8. Simulation of calibration polynomial at y-pixel 1233 and line 2. Four known positions of calibration planes depicted by blue stars.

4.7.2 Line Shifting Calibration

When scanning the lines, the x-pixel displacement can no longer be directly mapped to the depth. This is because each polynomial is only valid for the specific pixel, and by scanning the lines, the pixel changes. When scanning the lines, instead of fitting a polynomial to the depths for each pixel, a surface is fit to all lines across all depths for every y position on the image. This allows us to know the relationship between the x-pixel shift and depth for not only the line locations but also for locations between the lines. While this method of sometimes faster for data acquisition, it is less accurate because the data is being extrapolated rather than being directly measured. This can lead to incorrect approximations; however, this method is still accurate.

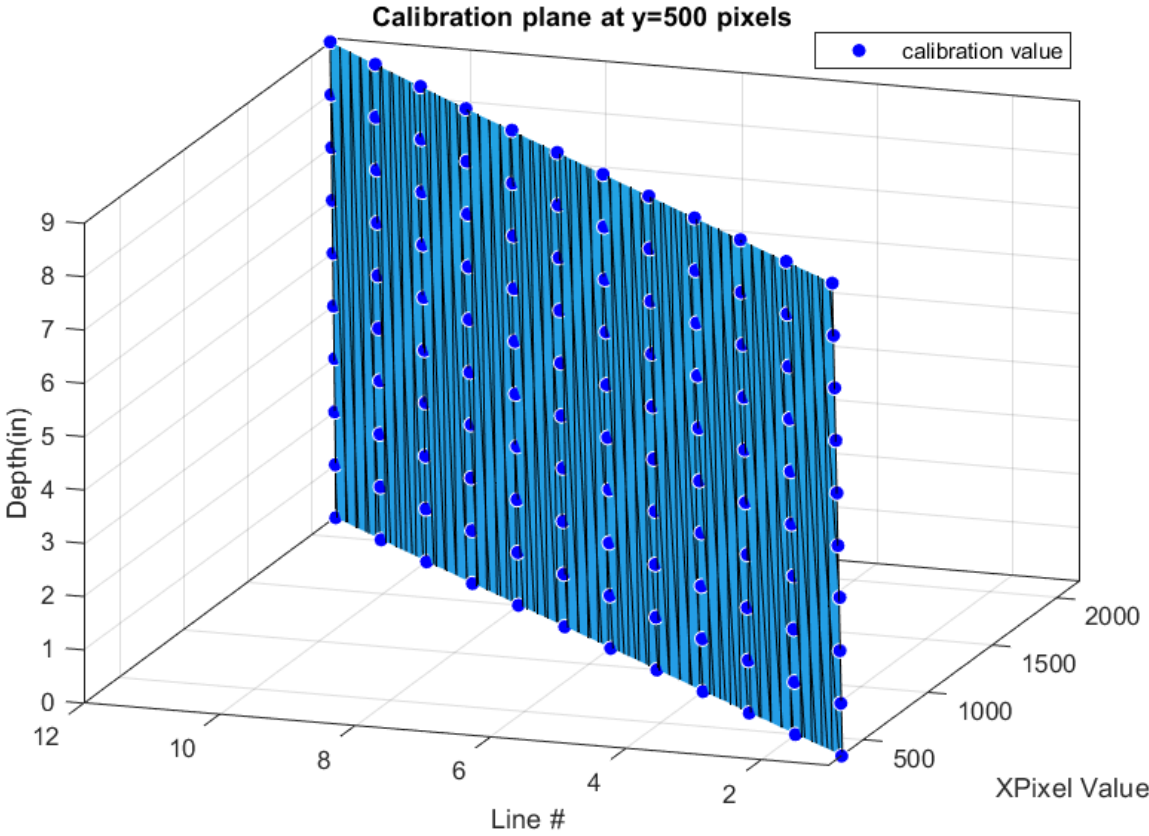


Figure 9. Simulation of calibration plane at y-pixel=500 for all lines. Known values from calibration are depicted by blue circles.

Figure 9 depicts a plane fit to the different x-pixel values and depths for all lines at y=500 pixels. The plane is fit to the known values obtained during calibration depicted by the blue dots. This plane can be used to fit any x-pixel value and line number to a depth, even if the line is between the calibrated line positions.

4.8 OBJECT FITTING

The same process used to determine the center of the lines for the calibration images is completed for the object images.

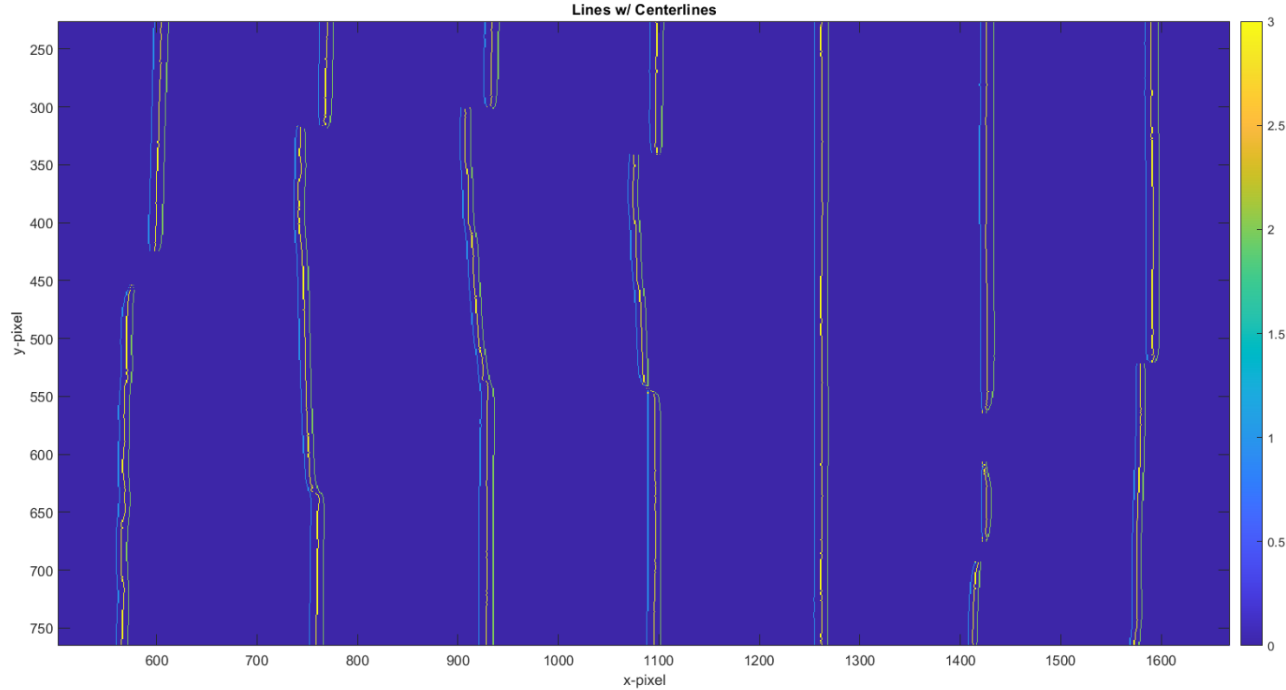


Figure 10. Simulation showing left border (=1, light blue), right border (=2, green), and center (=3, yellow) of calibration lines. Lines are offset, and gaps are present due to the object profile.

To assign positions to the lines, they need to be sorted. However, parts of the lines may be obstructed by the object, so a simple left-to-right count is not sufficient. To address this, each of the calibration lines is assigned a range of pixels based on their positions at minimum and maximum

depths. Ideally, the line at maximum depth is close to the subsequent line at minimum depth to maximize depth resolution. The ranges are determined by the mean location between the first line at maximum depth and the next line at minimum depth. With these pixel ranges, the object lines can be sorted, giving new x-pixel positions.

Once the centerline x-pixel positions are obtained, the values can be fit.

4.8.1 Object Fitting with No Shifting

In the image processing, each projected line for every row on the detector was given an x-pixel location. The new x-pixel position is fit to the polynomial line found in calibration. This gives a new z-value for that pixel. By combining the z-values for each pixel along the entire line, a profile of the object is obtained. Since multiple lines were used, multiple profiles along each line are obtained. Each profile's x and y positions correspond to the centerline values at the minimum depth calibration image.

4.8.2 Object Fitting with Object Shifting

The polynomial fitting procedure is completed for every shifted object image. To combine these profiles, the relative object position must be determined. Since known values include the distance between each shift and the distance required to shift a point on the object from one line to the next, the shifts can be scaled to the distance between lines. From here a point cloud is plotted combining the point clouds for all object-scanned images.

4.8.3 Object Fitting with Line Shifting

With the line shifting method, the line values are an input for object fitting. The lines values are assigned based off of the line pixel value relative to the calibration lines. For example, when five different scanning positions are used, the line values for the first image are [1.2, ...12], the second image are [1.2, 2.2, ...12.2], and the fifth image are [1.8, 2.8, ...12.8]. By inputting the x-pixel shift and line number, the z-value can be fit to the surface.

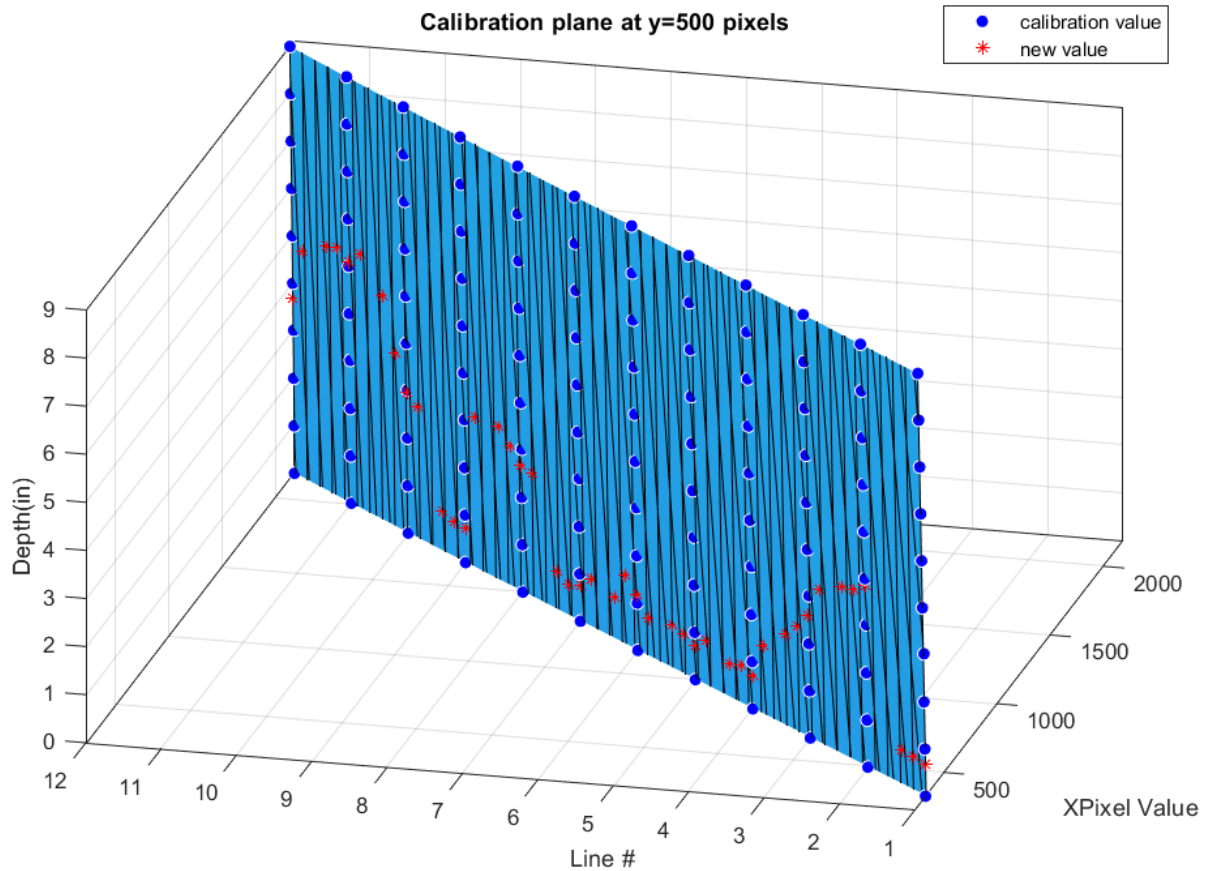


Figure 11. Simulation of calibration plane at y-pixel=500 for all lines. Known values from calibration are depicted by blue circles, and the new object values are depicted by red stars. The new depth values were found by fitting the line number and x-pixel values to the plane.

From here a point cloud is plotted combining the point clouds for all line-scanned images.

5. Results

5.1 3D POINT CLOUDS

In the end, 3D point clouds were successfully obtained using all three methods. For all results the background lines reflected off of the viewing screen have been removed by shifting the minimum depth to be greater than zero. This is done to make the images clearer.

5.1.1 Single Shot Point Cloud

A point cloud can be obtained in a single shot, however as discussed previously this results in a low density point cloud and is only suitable for capturing objects with less details. Because of this, this method is demonstrated using a plastic tube.

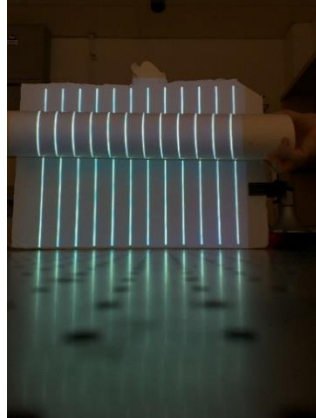


Figure 12. The raw image used for finding the 3D shape of the tube.

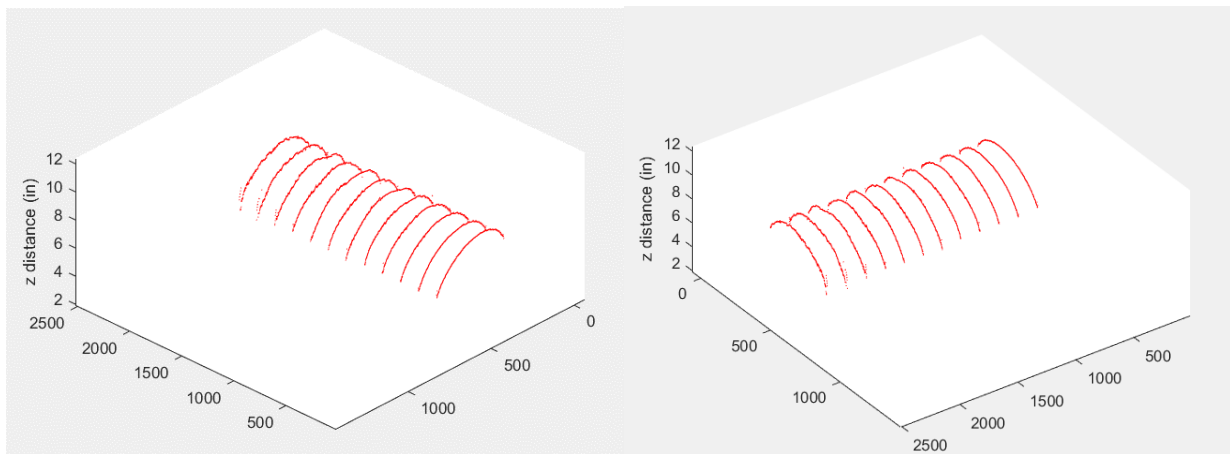


Figure 13. The right (shown left) and left (shown right) views of the 3D point clouds generated using the single-shot no scanning method.

5.1.2 Comparing Object-Shifted and Line-Shifted Point Clouds

Both object-shifting and line-shifting methods gave similar results when used on a plastic Einstein Face. This object was not ideal due to the high specular reflectivity, however using this object demonstrates the surprising level illumination variability of this method. This object was also used due to its lightweight nature making it ideal for the object shifting technique.



Figure 14. (left) The first image used for triangulation using both line shifting and object shifting methods.

Figure 15. (right) An image of the object used.

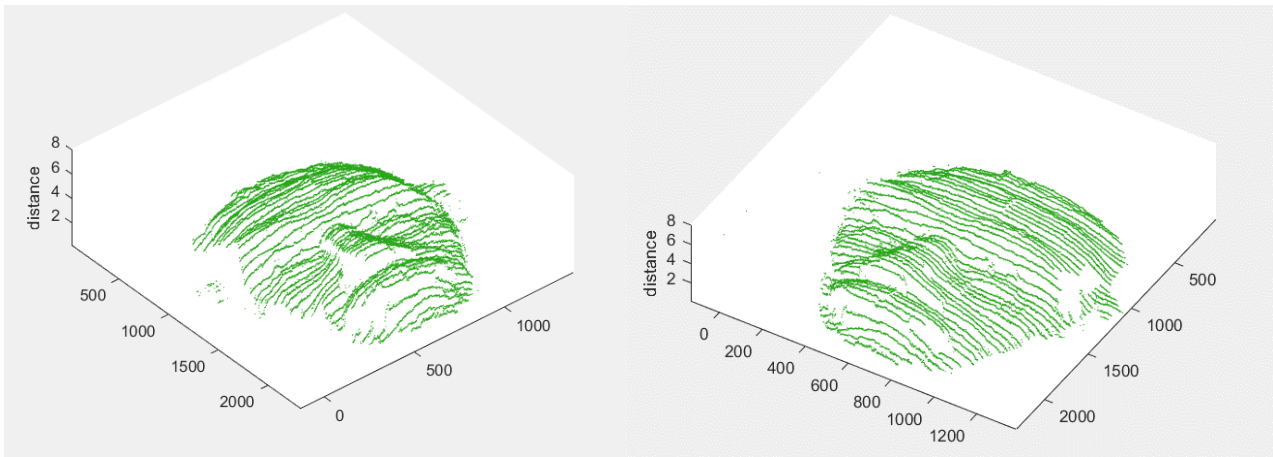


Figure 16. The left (shown left) and right (shown right) views of the 3D point clouds generated using the object shifting method.

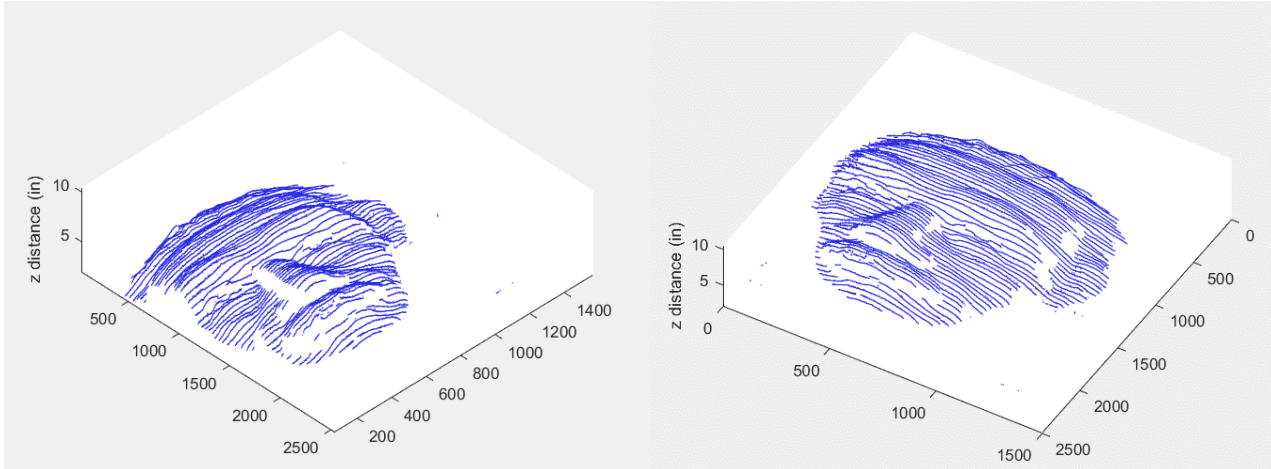


Figure 17. The left (shown left) and right (shown right) views of the 3D point clouds generated using the line shifting method.

As shown in Figures 16 and 17, both object-shifting and line-shifting methods offer similar results by visual assessment. While the calibration plane used in the line-shifting method proved to be less accurate, this error did not have any extreme effects when creating a point cloud. In fact, additional errors are added. When shifting the object, the distances were determined using a ruler which has an error of about 1.6 mm. Furthermore, when the object was shifted the angle of the object also experienced minor adjustments.

In both point clouds there appears to be a gap next to the nose of the object when viewed from the left side. This happens when the object has a steep change in the z distance, and the data for this area is covered by the tall object next to it. These gaps can be minimized by decreasing the baseline distance; however, this comes with additional tradeoffs.

5.1.3 Line Shifted Point Cloud

The Line-shifting method works best for heaving objects. Figure 20 depicts a 3D point cloud of a heavy object.



Figure 18. (left) The first image used for triangulation of heavy object using line-shifting method.

Figure 19. (right) An image of the heavy object used.

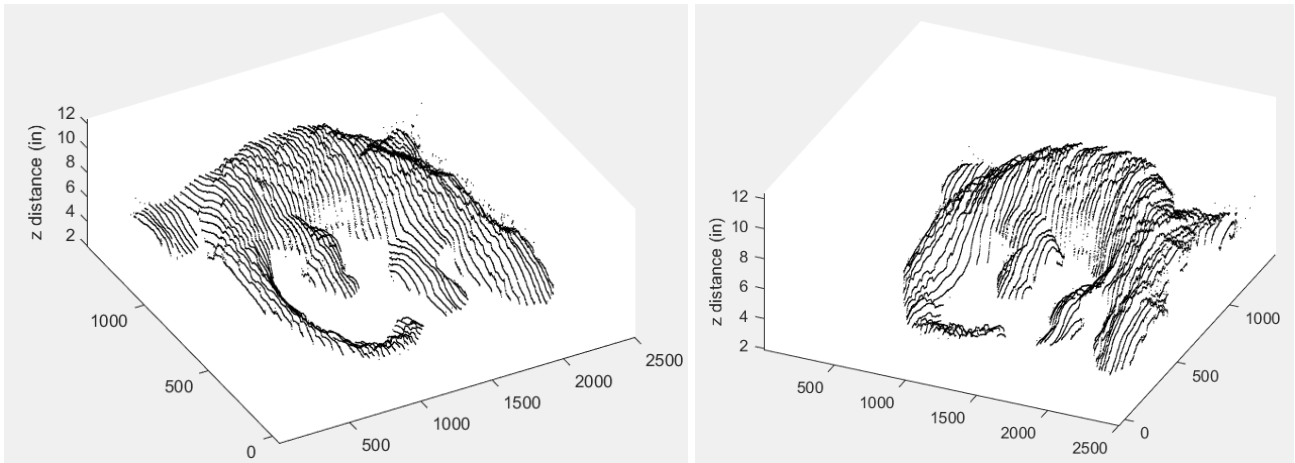


Figure 20. The left (shown left) and right (shown right) views of the 3D point clouds generated using the line shifting method for a heavy object.

These point clouds appear to be accurate to the object. There is some random noise especially near the right edge of the object. In Figure 20 the stripes on the back of the lizard can almost be made out but are not clear. These stripes have a depth of approximately 12 mm.

5.2 CALIBRATION LINE VS. CALIBRATION PLANE ERROR

There were two calibrations discussed depending on image acquisition: utilizing a calibration curve or calibration plane. The two different calibration methods can be assessed by imaging the planar surface used for calibration at a known location. The object is simple enough to be evaluated in a single shot, and therefore no scanning is required. This allows the same input data for both the calibration curve and plane to be used. Eight calibration images were captured at depths of 0, 25.4, 50.8, 76.2, 127, 152.4, 177.8, and 203.2 millimeters. The test image was of a planar surface located at 101.6 millimeters.

The results are shown in Figure 21 and Figure 22. The error is shown in Figure 23.

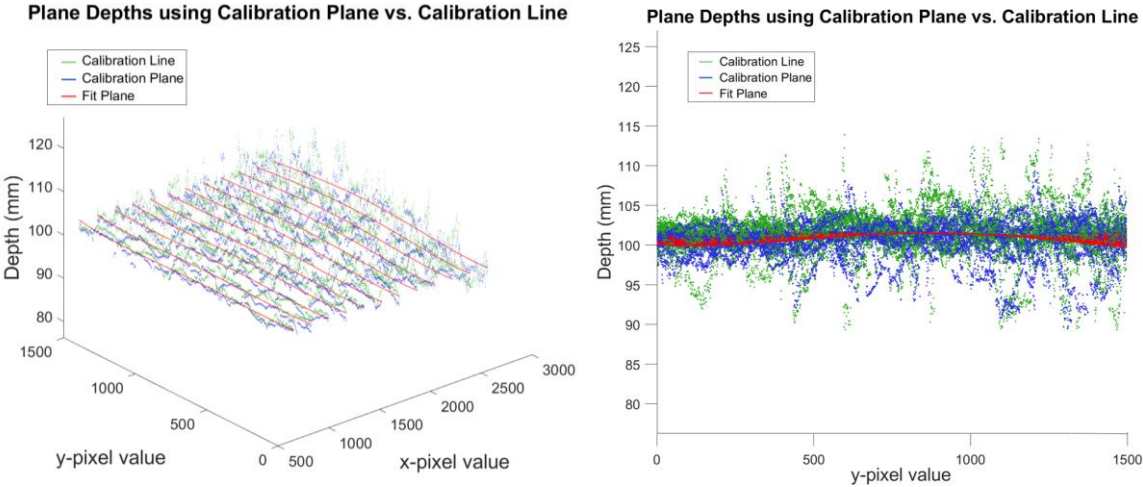


Figure 21. (left) shows the depth values found using both a calibration line (green) and calibration plane (blue), as well as a plane of best fit (red). This figure demonstrates the general shape of the plane.

Figure 22. (right) shows the depth values found using both a calibration line and calibration plane viewed from the side. This figure demonstrates the general cluster around the plane of best fit with a few outliers.

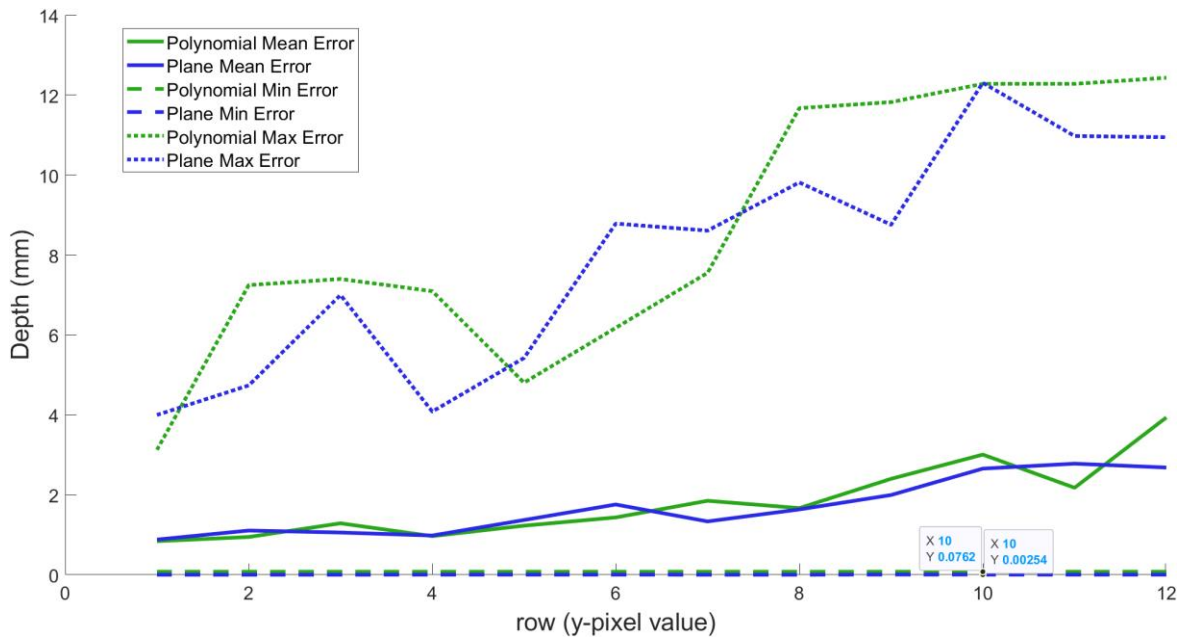


Figure 23. shows the minimum, mean, and maximum error for using the calibration line compared to the calibration plane. The minimum error is depicted by the dashed lines, the mean error is shown with the solid lines, and the maximum error is shown by the dotted lines.

Error values are shown in Figure 23. These values are determined by comparing the raw values to the plane of best fit. The maximum error values are very high, on the order of 4-12 mm, however these are outliers and do not remove a significant amount of structure from the 3D point cloud. The mean errors are fairly low at 1-3 mm and the minimum errors are extremely low at 0-0.1 mm.

The measured plane using the calibration curve method had an average depth of 101.519 mm and a standard deviation of 0.98 mm, while the calibration plane method resulted in an average depth of 100.64 mm and a standard deviation of 0.66 mm. Although the calibration curve method is closer to the expected location of the plane, it has more variability. Since the ruler used for the measurement has an error of 1.6 mm, it cannot be confidently determined that the depth determined from the polynomial was more accurate. Therefore, the calibration plane method is the preferred method due to its lower deviation.

It is also important to acknowledge that this is data for one test plane using one set of calibration images. By optimizing the calibration photos, less error may be possible for both methods. Also, by changing the test plane the error could increase or decrease for both methods.

6. Conclusion

A system for projected multi-line triangulation was successfully created to be used for educational applications. The system was created to be accessible, only requiring commonly available materials such as a cell phone and projector. It was also designed for high simplicity, utilizing basic triangulation principles, and using visible light so that the measurement offset can be observed. It is capable of utilizing three different image acquisition methods: no scanning, object scanning and line scanning. When no scanning or object scanning was used, the depths were calibrated using a polynomial curve. When line scanning was used, the depths were calibrated using a polynomial plane. When tested at a specific plane, the calibration curve had a standard deviation of 0.98 mm and the calibration plane method had a standard deviation of 0.66 mm. Therefore, using the calibration plane is the preferred method. Using all methods, 3D point clouds of various objects were successfully produced. These point clouds did not have high depth resolution; however, they were precise enough to capture details with depths of 12 mm.

There are many areas of future research regarding this project. While this system was able to capture depths of 12 mm, it may be interesting to explore ways to increase this depth resolution by experimenting with different projectors or more advanced calibration techniques. It would also be useful to increase the simplicity of the system by adding a user interface so that the system could be used without prior knowledge of Matlab.

7. REFERENCES

1. F. Willomitzer, "Lecture 19: Triangulation," The University of Arizona, Wyant College of Optical Sciences (2023).
2. "3D sensor market by type (image sensor, accelerometer sensor, position sensor, and others), technology (structured light, time of flight, Stereoscopic Vision, ultrasound, and others), connectivity (Wireless and Wired), and end use (consumer electronics, healthcare, Aerospace & Defense, automotive, and others): Global Opportunity Analysis and Industry Forecast, 2022-2031," Market Research Firm, <<https://www.researchdive.com/89/3d-sensor-market>> .
3. S. Vaskevich, "What is 3D Imaging Technology? how does it work?," CyberFox Agency What is 3D imaging technology How does it work Comments, <<https://cyberfox.net/blog/what-is-3d-imaging-technology/#:~:text=3D%20imaging%20technology%20has%20many%20uses.,for%20engineering%20and%20manufacturing%20purposes>>.
4. Zivid, 3D vision technology principles, <<https://www.zivid.com/3d-vision-technology-principles>>.
5. R. L. Mendez, "The rise of depth on mobile," Graphics, Gaming, and VR blog - Arm Community blogs - Arm Community, <<https://community.arm.com/arm-community-blogs/b/graphics-gaming-and-vr-blog/posts/the-rise-of-depth-on-mobile>> .
6. M. Alfonso, "3D scanning with Structured Light," Bitfab, 22 September 2020, <<https://bitfab.io/blog/3d-structured-light-scanning/>>.
7. K. Kamani, "Types of 3D scanning technologies and 3D scanners," LinkedIn, <<https://www.linkedin.com/pulse/types-3d-scanning-technologies-scanners-karan-kamani/>>.
8. "Apple," Official Apple Support, <https://support.apple.com/kb/SP804?locale=en_US>
9. "Halide mark II: Pro. camera. action.," Halide, <<https://halide.cam/>>.
10. "VS250 SVGA 3LCD Projector," V11H838220 | VS250 SVGA 3LCD Projector | Portable | Projectors | For Work | Epson US, <[https://epson.com/For-Work/Projectors/Portable/VS250-SVGA-3LCD-Projector/p/V11H838220#:~:text=Featuring%20SVGA%20resolution%20\(800%20x,and%20running%20in%20no%20time](https://epson.com/For-Work/Projectors/Portable/VS250-SVGA-3LCD-Projector/p/V11H838220#:~:text=Featuring%20SVGA%20resolution%20(800%20x,and%20running%20in%20no%20time)>.












Master's Report Approval

Final Audit Report

2023-05-11

Created:	2023-05-10
By:	Madeline Bergay (mbergay@arizona.edu)
Status:	Signed
Transaction ID:	CBJCHBCAABAAY78xzDbsfjXOrOpZGZnS7mlQkzuXsED2

"Master's Report Approval" History

-  Document created by Madeline Bergay (mbergay@arizona.edu)
2023-05-10 - 1:28:24 AM GMT
-  Document emailed to hhua@optics.arizona.edu for signature
2023-05-10 - 1:31:26 AM GMT
-  Email viewed by hhua@optics.arizona.edu
2023-05-10 - 4:49:10 AM GMT
-  Signer hhua@optics.arizona.edu entered name at signing as /Hong Hua/
2023-05-10 - 4:49:41 AM GMT
-  Document e-signed by /Hong Hua/ (hhua@optics.arizona.edu)
Signature Date: 2023-05-10 - 4:49:43 AM GMT - Time Source: server
-  Document emailed to Thomas Milster (milster@arizona.edu) for signature
2023-05-10 - 4:49:45 AM GMT
-  Email viewed by Thomas Milster (milster@arizona.edu)
2023-05-10 - 2:40:35 PM GMT
-  Document e-signed by Thomas Milster (milster@arizona.edu)
Signature Date: 2023-05-10 - 2:40:59 PM GMT - Time Source: server
-  Document emailed to Florian Willomitzer (fwillomitzer@arizona.edu) for signature
2023-05-10 - 2:41:01 PM GMT
-  Email viewed by Florian Willomitzer (fwillomitzer@arizona.edu)
2023-05-11 - 11:47:27 PM GMT
-  Document e-signed by Florian Willomitzer (fwillomitzer@arizona.edu)
Signature Date: 2023-05-11 - 11:48:46 PM GMT - Time Source: server

✔ Agreement completed.

2023-05-11 - 11:48:46 PM GMT